# An Appearance-Like Reactor Experiment To Measure $U_{e3}$

José Bernabéu<sup>1</sup> and Sergio Palomares-Ruiz<sup>1,2,3</sup>

<sup>1</sup> Departamento de Física Teórica and IFIC, Universidad de Valencia-CSIC, 46100 Burjassot, Valencia, Spain

<sup>2</sup> Department of Physics and Astronomy, UCLA, Los Angeles, CA 90095, USA

<sup>3</sup> Department of Physics and Astronomy, Vanderbilt University, Nashville TN 37235, USA

# Abstract

Conventional reactor neutrino experiments are dissapearance experiments, and thus have less sensitivity to small mixing angles than appearance experiments do. It has been recently shown that future reactor neutrino experiments consisiting of a near and far detector are competitive with first-generation superbeams in order to determine  $\sin^2 2\theta_{13}$  down to  $10^{-2}$ . We show that by using the antineutrino-electron elastic scattering at the near detector around the configuration where  $d\sigma^{\overline{\nu}_e}/dT$  presents a dynamical zero, an appearance-like experiment can be simulated, with a sensitivity comparable to the one achieved with the inverse  $\beta$ -decay reaction in the far detector. Thus, the near detector could also be used to look for oscillations. We present how antineutrinoelectron elastic scattering could be properly used for this purpose allowing that the combination of the measurements in the far detector and in the near detector would push the sensitivity of the experiment to a lower value of  $\theta_{13}$ .

PACS numbers: 14.60.Pq, 13.15.+g, 28.41.-i

FTUV-03-1111, IFIC-03-51

# I. INTRODUCTION

The old solar and atmospheric neutrino problems are coming to an end and we are entering an era of precision experiments. During the last years, different results have given strong evidences of solar and atmospheric neutrino oscillations [1, 2]. Recently, the LMA solution of the solar neutrino problem was confirmed by the KamLAND reactor experiment [3] and also by more data from SNO [4]. The allowed regions for the solar and atmospheric square mass differences and mixing parameters are, thus, getting very constrained. We do not know, however, one very important question: whether  $\theta_{13}$ , i.e., the  $U_{e3}$  mixing, is different from zero. This mixing is the door to the experimental measurement of fundamental CP (or T) violation effects [5], the type of mass hierarchy [6, 7, 8] and controls the Earth matter effect in supernova neutrino oscillations (see, e.g., Refs. [9]). Besides the experimental implications, the smallness of  $\theta_{13}$  [10, 11], compared to the other two mixing angles (in a three-neutrino mixing scheme), which are relatively large [1, 2, 3], is something not yet explained from the theoretical point of view.

The CHOOZ reactor experiment provides the more stringent bounds on the value of  $\theta_{13}$  [10], although there are several experiments consisting on conventional beams like K2K [12], MINOS [13] or CNGS experiments [14], which could establish  $\theta_{13} \neq 0$  or improve the present lower limit,  $\sin^2 2\theta_{13} < 0.10$ . Even better limits are foreseen with superbeams [15] or neutrino factories [16].

When talking about controlled neutrino oscillation experiments, there are essentially two types of them: appearance and disappearance experiments. In an appearance experiment, a neutrino of a given flavor is produced. During the propagation, its flavor changes and it is detected via a pure charged current reaction. On the other hand, in a disappearance experiment a neutrino of a definite flavor is produced in a controlled way and the depletion in the original flux after propagation is the signal for oscillation. The decrease in the original flux is measured via charged current reactions which see the same flavor as the one produced. However, for small mixings, the main signal in the detector comes from neutrinos of the same flavor as the one produced, so this means that there is less sensitivity to small mixings for disappearance experiments. In addition, charged current detection has a threshold energy for production, so that it is, in general, impossible to use low energy neutrinos for appearance experiments. It has been recently proposed [17, 18] the use of reactor neutrinos to improve the sensitivity to  $\theta_{13}$ . In order to do this, two detectors have to be used, a near detector and a far detector. The latter at a distance of ~ 1.7 km and the former nearer so that no oscillations take place. In this way, systematic errors can be reduced and a sensitivity down to  $\sin^2 2\theta_{13} \simeq 0.01 - 0.02$  could be reached.

Nuclear reactors produce low energy  $\overline{\nu}_e$  and the basic detection reaction is the inverse  $\beta$ -decay which has an energy threshold of 1.806 MeV [19]. For these energies a baseline of  $\gtrsim 1$  km is needed so that oscillations can take place for the atmospheric square mass difference. This is, however, a disappearance experiment and thus, less sensitive to small mixings, which is the case.

We would like to find an experiment capable of measuring very small mixings. In order to accomplish this task, we will focus on the following mixed charged and neutral current reaction:  $\overline{\nu}_e + e^- \rightarrow \overline{\nu}_e + e^-$ . We will make use of the fact that for another flavor,  $\overline{\nu}_x + e^- \rightarrow \overline{\nu}_e + e^-$ .  $\overline{\nu}_x + e^-$  (with  $x \neq e$ ) is a pure neutral current reaction. Consequently, the cross sections for these reactions are different. In principle, this fact could be used to perform a neutrino oscillation experiment  $(\overline{\nu}_e \to \overline{\nu}_x)$  which would be a mixture of appearance and disappearance experiments. This mixture depends on the neutrino energy and the electron recoil direction, so it could be tuned by the choice of the appropriate kinematics. If oscillations take place, the number of recoil electrons will be different from the case of no oscillations. However, if both cross sections are similar, the effect has a minor impact on the study of oscillations. Nevertheless, it is known [20] that the cross section for the scattering of electron antineutrinos on electrons presents a destructive interference and a dynamical zero for the kinematic configuration corresponding to an incident antineutrino energy,  $E_{\nu} = \frac{m_e}{4\sin^2\theta_W} \simeq m_e$ , and maximum recoil energy  $T = T_{max} = \frac{2E_{\nu}^2}{2E_{\nu}+m_e} \simeq \frac{2m_e}{3}$  (forward electron). The point here is that this zero is not present in  $\overline{\nu}_x + e^- \rightarrow \overline{\nu}_x + e^-$  and this fact could make possible to perform an appearance-like experiment. Indeed, if we were able to select only the events in a window around the dynamical zero configuration, we would be detecting almost only  $\overline{\nu}_x$ and not  $\overline{\nu}_e$  which would be a sort of appearance-like experiment. We will take advantage of these facts in order to study the possibilities of using this channel to measure (or to get more restrictive bounds on)  $U_{e3}$ . For typical antineutrino energies in a reactor, the inverse  $\beta$ -decay reaction is the dominant one and the cross section for  $\overline{\nu} + e \rightarrow \overline{\nu} + e$  is less than 1% that of  $\overline{\nu}_e + p \rightarrow e^+ + n$ . Nevertheless, neutrino-elastic scattering has no energy threshold

and the reactor neutrino flux has a maximum at ~ 0.5–1.0 MeV. Keeping all this in mind, we will show that the near detector could be used to search for oscillations in this channel, and not only to reduce systematic errors in the far detector. Therefore, the combination of the measurement in the near and in the far detectors might improve the sensitivity to  $\theta_{13}$ . The main purpose of this paper is to motivate this channel as a suitable way to look for oscillations in the near detector.

It is important to remark several additional facts which explain why it is worthwhile to study more carefully this sort of appearance-like experiment by means of the  $\overline{\nu}_e - e^$ reaction:

- i) The dynamical zero is only present for  $\bar{\nu}_e$ , not for  $\nu_e$  or  $\nu_\mu$  ( $\bar{\nu}_\mu$ ),  $\nu_\tau$  ( $\bar{\nu}_\tau$ ).
- ii) The flavour  $\bar{\nu}_e$  is precisely the one which is produced copiously in nuclear reactors.
- iii) The neutrino energy at which the zero appears is around the peak of the antineutrino reactor spectrum [21, 22].
- iv) The dynamical zero is located at the maximum electron recoil energy  $T \simeq 2m_e/3$ . This value is in the range of the proposed experiments [23] to detect recoil electrons.

The outline of the paper is the following. In section II, we present the framework of neutrino oscillations. In section III we present the basics of the far detector measurement. In section IV, we analyze the optimal baseline for the near detector in order to be sensitive to neutrino oscillations working as an appearance experiment. The sensitivity to  $\theta_{13}$ , comparatively as what can be done just with the far detector, is studied. Finally, in section V, we present our conclusions.

# **II. REACTOR NEUTRINO OSCILLATIONS**

In the case of reactor neutrino experiments we are dealing with short baselines and thus, when considering neutrino oscillations, we can safely neglect matter effects. The form for the survival probability is then given by

$$P_{\bar{\nu}_e \to \bar{\nu}_e} = 1 - \cos^4 \theta_{13} \sin^2 2\theta_{12} \sin^2 \left(\frac{\Delta m_{21}^2 L}{4E}\right)$$

$$+\sin^2 2\theta_{13} \left[\cos^2 2\theta_{12} \sin^2 \left(\frac{\Delta m_{31}^2 L}{4E}\right) + \sin^2 \theta_{12} \sin^2 \left(\frac{\Delta m_{32}^2 L}{4E}\right)\right]$$
(2.1)

Considering  $\sin^2 2\theta_{13}$  and  $\sin^2 \left(\frac{\Delta m_{21}^2 L}{4E}\right)$  small, to the first order in this approximation we can write Eq. (2.1) as

$$P_{\bar{\nu}_e \to \bar{\nu}_e} \simeq 1 - \left[\sin^2 2\theta_{13} \sin^2 \left(\frac{\Delta m_{31}^2 L}{4E}\right) + \sin^2 2\theta_{12} \sin^2 \left(\frac{\Delta m_{21}^2 L}{4E}\right)\right]$$
(2.2)

If the high  $\Delta m_{21}^2$  solution, with  $\Delta m_{21}^2 \sim 10^{-4} \text{ eV}^2$ , had turned out to be the right one, special care for the second term in the bracket in Eq. (2.2) would have been needed. In this case the determination of  $\theta_{13}$  and  $\theta_{12}$  are coupled, and a joint analysis of reactor antineutrino experiments with baseline of about 1 km and KamLAND would be needed (see Ref. [24] for a study of the impact of  $\theta_{13} \neq 0$  on KamLAND data). The new SNO salt phase data [4], however, strogly points towards the low  $\Delta m_{21}^2$  solution.

From the simplycity of Eq. (2.2) it is easily seen that correlations and degeneracies play a minor role in these type of experiments. However, this means that there exist some limitations, as it is the fact that there is no dependence on the atmospheric neutrino mixing  $\theta_{23}$ , on the type of hierarchy (sign of  $\Delta m_{31}^2$ ) or on the CP violating phase.

Throughout the paper we will use the following values for the different neutrino oscillation parameters [1, 4]:

$$\Delta m_{21}^2 = 7.1 \times 10^{-5} \text{eV}^2 \quad ; \ \Delta m_{31}^2 = 3.0 \times 10^{-3} \text{eV}^2 \quad ; \ \tan^2 \theta_{12} = 0.41 \tag{2.3}$$

The bracket in Eq. (2.2), giving the appearance probability,  $P_{\bar{\nu}_e \to \bar{\nu}_x}$   $(x \neq e)$ , shows its sensitivity to small values of the mixing angle  $\theta_{13}$ , unlike the case of the disappearance channel.

#### III. FAR VS NEAR DETECTOR

We will first consider the basics of the far detector reaction and the use of the elastic antineutrino-electron scattering in the near detector.

In order to reach a good sensitivity to  $\sin^2 2\theta_{13}$ , the detection of small spectral distortions in the positron event rates due to antineutrino oscillations is important. This is only possible by selecting an optimized baseline and by reducing systematic uncertainties to the level of 1%. These two points are crucial if we want to achieve an order of magnitude of improvement for the  $\sin^2 2\theta_{13}$  sensitivity. In the case of the far detector the dominant detection reaction is the inverse  $\beta$ -decay

$$\overline{\nu}_e + p \longrightarrow e^+ + n \qquad (E_\nu)_{th} = 1.804 \text{ MeV}$$
(3.1)

The selection of the proper baseline which gives the first oscillation maximum for reactor antineutrinos, directly follows from the typical energies of the inverse  $\beta$ -decay reaction, i.e., 3.5–4.0 MeV. As we will see below, for  $\Delta m_{31}^2 = (2.5 - 3.0) \times 10^{-3} \text{ eV}^2$  the optimum baseline is ~ 1.7 km.

We assume a far detector technology like the CHOOZ or KamLAND detectors and a typical integrated luminosity of  $\mathcal{L} = 8000 \text{ t} \cdot \text{GW} \cdot \text{yr}$ . For concreteness, in the case of the Kashiwazaki-Kariwa nuclear power plant whose maximum thermal power is 24.3 GW, and a 100-ton detector, an exposure-time of ~ 3.3 years would represent that luminosity.

Reaction (3.1) has a easily recognizable signal, the positron anihilation with an electron, in delayed coincidence with the  $\gamma$ -ray from the neutron capture. The energy of the positron is given by

$$E_{e^+} = E_{\overline{\nu}_e} - (M_n - M_p) + O(E_{\overline{\nu}_e}/M_n) \simeq E_{\overline{\nu}_e} - 1.293 \text{ MeV}$$
(3.2)

The visible energy in the detector is given by the sum of the positron energy plus the mass of the anihilated electron,  $E_{vis} = E_{e^+} + 0.511$  MeV. Therefore, a precise measurement of  $E_{vis}$  corresponds to a precise determination of the neutrino energy,  $E_{\bar{\nu}_e}$ . Considering constant detector efficiency,  $\epsilon$ , the expected number of events in the detector is given by

$$N = \mathcal{N}_p \times \mathcal{T}_{exp} \times \epsilon \times \frac{1}{4\pi L^2} \times \int \frac{d\Phi}{dE_{\overline{\nu}_e}} (E_{\overline{\nu}_e}) \cdot \sigma(E_{\overline{\nu}_e}) \cdot P_{\overline{\nu}_e \to \overline{\nu}_e}(E_{\overline{\nu}_e}) \cdot dE_{\overline{\nu}_e}$$
(3.3)

where  $\mathcal{N}_p$  is the number of protons in the detector,  $\mathcal{T}_{exp}$  is the exposure-time, L is the reactor-detector distance,  $d\Phi/dE_{\overline{\nu}_e}(E_{\overline{\nu}_e})$  is the initial reactor energy spectrum,  $\sigma(E_{\overline{\nu}_e})$  is the cross section for inverse  $\beta$ -decay and  $P_{\overline{\nu}_e \to \overline{\nu}_e}(E_{\overline{\nu}_e})$  is the survival  $\overline{\nu}_e$  given by Eq. (2.2).

The shape of the spectrum can be derived from a phenomenological parameterization of the spectra from several of short baselines experiments [22]

$$\frac{d\Phi}{dE_{\overline{\nu}_e}} = e^{a_0 + a_1 E_{\overline{\nu}_e} + a_2 E_{\overline{\nu}_e}^2} \tag{3.4}$$

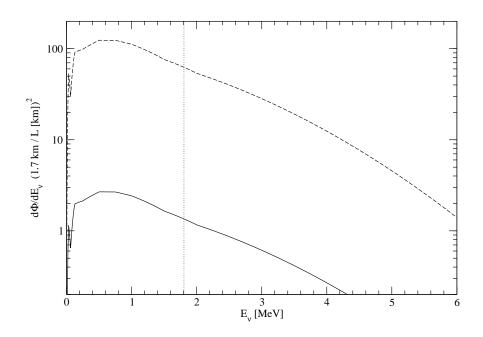


FIG. 1: Antineutrino nuclear reactor flux weighted by flux square-distance factor relative to the far detector at 1.7 km. Near detector at 0.25 km (dashed line) and far detector at 1.7 km (solid line) from the reactor.

where the values of the energy coefficients depend on the parent nuclear isotope. This expression is a very good approximation for antineutrino energies above 2 MeV. For lower energies, we have used a calculation based on a summation of the allowed shape  $\beta$  decays of all fission fragments. The coefficients of Eq. (3.4) and the calculated spectra for lower energies are given in Ref. [21]. In addition, we assume a constant chemical composition for the reactor, 53.8% of <sup>235</sup>U, 32.8% of <sup>239</sup>Pu, 7.8% of <sup>238</sup>U and 5.6% of <sup>241</sup>Pu (see, e.g., Refs. [24, 25]). We will also consider the thermal energy associated with the fissioning of each of those nuclei as given in Ref. [26], that is 201.7 MeV for <sup>235</sup>U, 205.0 MeV for <sup>239</sup>Pu, 210.0 MeV for <sup>238</sup>U and 212.4 MeV for <sup>241</sup>Pu.

In Fig. 1, we show the antineutrino nuclear reactor flux for the near (dashed curve) and far (solid curve) detector distances to the reactor, weighted by the flux square-distance factor in each detector. As can be seen from the figure, the nuclear reactor flux presents a maximum around  $E_{\overline{\nu}} \simeq 0.5$ –1.0 MeV, which it is roughly a factor of seven with respect to the relevant energies in the far detector,  $E_{\overline{\nu}} = 3.5$ –4.0 MeV. Thus, we have taken 1.7 km and 0.25 km ( $\simeq$  1.7 km/7) for the far and near detector-reactor distances, respectively. The inverse  $\beta$ -decay

reaction is only sensitive to antineutrino energies higher than the threshold one, 1.806 MeV (limited by the dotted line), while the antineutrino-electron elastic reaction is so for the entire spectrum. In addition, as can be seen from Fig. 1, within the region of the maximum, the nuclear reactor flux is a few times larger than for the relevant energies detected by the inverse  $\beta$ -decay reaction in the far detector. All in all, due to being closer to the nuclear reactor and working in a higher-flux region, the spectrum around the maximum in the near detector is a factor ~ 100 times larger than the part of it sensitive to the inverse  $\beta$ -decay in the far detector. This can be understood by comparing the dashed and solid lines in Fig. 1.

On the other hand, there are different calculations of the cross section for the inverse  $\beta$ -decay which take into account different approximations valid for different regimes [27]. To the lowest order, this cross section is given by

$$\sigma(E_{e^+}) = \frac{2\pi^2}{m_e^5 f \tau_n} p_{e^+} E_{e^+}$$
(3.5)

where f is the phase space factor for the free neutron decay and  $\tau_n$  is the lifetime of a free neutron.

Although the cross section for  $\overline{\nu} + e \rightarrow \overline{\nu} + e$  is about 1% that of  $\overline{\nu}_e + p \rightarrow e^+ + n$ , the flux gain, discussed before, due to the use of the near detector around the maximum of the spectrum compensates this factor. Therefore, we expect, roughly, a similar number of events in the far detector using the inverse  $\beta$ -decay reaction and in the near detector using the antineutrino-electron elastic scattering<sup>1</sup>.

Thus, as the mixing  $\theta_{13}$  is small and the far detector performs a disappearance experiment, it is very important to reduce systematic uncertainties. The near detector will help in this task using the same reaction as the far detector, but it will also be useful to perform neutrino oscillation studies by itself using antineutrino-electron elastic scattering.

### **IV. APPEARANCE-LIKE EXPERIMENT**

Many of the systematic uncertainties, due to poor knowledge of the neutrino flux, number of protons and detection efficiency cancel out if besides a far detector, a near detector is used and measurements in both detectors are compared. It has been recently shown [17, 18] that

<sup>&</sup>lt;sup>1</sup> Assuming similar masses for both detectors.

the use of a near detector at ~ 0.2 km makes possible the determination of  $\sin^2 2\theta_{13}$  down to 0.01–0.02. It has also been shown that reactor measurements can play a role complementary to long baseline experiments, helping to resolve parameter degeneracies.

As we have already argued above, we will show that not only is the near detector useful to lower the systematic uncertainties, but also to perform neutrino oscillation measurements complementary to those in the far detector, by using antineutrino-electron elastic scattering for energies around the maximum of the reactor antineutrino spectrum, which, combined with the smaller baseline, implies a flux gain of ~ 100 with respect the far detector measurements. Thus, although the antineutrino-electron elastic cross section is a factor ~ 100 smaller than in the case of inverse  $\beta$ -decay, working on the maximum of the reactor spectrum, allows us to use this reaction for neutrino oscillation studies in the near detector.

The main purpose of using the antineutrino-electron elastic scattering as the detection reaction is to simulate an appearance experiment. In order to achieve this, only that part of the recoil electron spectrum around the dynamical zero [28] must be considered. For this channel, the number of events is given by

$$N = \mathcal{N}_p \times \mathcal{T}_{exp} \times \epsilon \times \frac{1}{4\pi L^2} \times \int \frac{d\sigma^{\overline{\nu}}}{dT} (E_{\overline{\nu}_e}, T) \cdot \frac{d\phi^o}{dE_{\overline{\nu}_e}} (E_{\overline{\nu}_e}) \cdot dE_{\overline{\nu}_e} \, dT \tag{4.1}$$

where  $\frac{d\sigma^{\overline{\nu}}}{dT}(E_{\overline{\nu}_e},T)$  is the sum of all the cross sections convoluted with the oscillation probabilities<sup>2</sup>

$$\frac{d\sigma^{\overline{\nu}}}{dT}(E_{\overline{\nu}_e},T) = P_{\overline{\nu}_e \to \overline{\nu}_e}(E_{\overline{\nu}_e}) \frac{d\sigma^{\overline{\nu}_e}}{dT}(E_{\overline{\nu}_e},T) + P_{\overline{\nu}_e \to \overline{\nu}_x}(E_{\overline{\nu}_e}) \frac{d\sigma^{\overline{\nu}_x}}{dT}(E_{\overline{\nu}_e},T)$$
(4.2)

The first term in Eq. (4.2), the dissapearance term, is the one measured in the far detector, but it cannot be substracted out because the energies of interest in the near detector are much lower for the elastic reaction. Around the dynamical zero,  $d\sigma^{\bar{\nu}_e}/dT = 0$ , and Eq. (4.2) shows that around this point, this reaction simulates an appearance-like experiment.

Using the fact that the probability of  $\overline{\nu}_e$  going to an antineutrino of any flavor must be equal to one, we can rewrite Eq. (4.2) as

<sup>&</sup>lt;sup>2</sup> We are taking the differential cross sections for  $\overline{\nu}_{\mu}$  and  $\overline{\nu}_{\tau}$  ( $\overline{\nu}_{x}$ ) as equal, not considering radiative corrections.

$$\frac{d\sigma^{\overline{\nu}}}{dT}(E_{\overline{\nu}_e},T) = \frac{d\sigma^{\overline{\nu}_e}}{dT}(E_{\overline{\nu}_e},T) + \left(\frac{d\sigma^{\overline{\nu}_x}}{dT}(E_{\overline{\nu}_e},T) - \frac{d\sigma^{\overline{\nu}_e}}{dT}(E_{\overline{\nu}_e},T)\right) P_{\overline{\nu}_e \to \overline{\nu}_x}$$
(4.3)

The antineutrino-electron elastic scattering cross sections are given by [21]

$$\frac{d\sigma^{\overline{\nu}_i}}{dT}(E_{\overline{\nu}_i},T) = \frac{2\,G_F\,m_e}{\pi} \left[ (g_R^i)^2 + (g_L^i)^2 \,\left(1 - \frac{T}{E_{\overline{\nu}_i}}\right)^2 - g_L^i \,g_R^i \,\frac{m_e\,T}{E_{\overline{\nu}_i}^2} \right] \tag{4.4}$$

where  $G_F$  is the Fermi coupling constant, T the recoil kinetic energy of the electron and  $E_{\overline{\nu}_i}$ the antineutrino incident energy. For neutrinos one has to make the change  $g_L^i \leftrightarrow g_R^i$ . In terms of the weak mixing angle  $\theta_W$ , the chiral couplings  $g_L^i$  and  $g_R^i$  can be written for each neutrino flavor as

$$g_L^e = \frac{1}{2} + \sin^2 \theta_W \qquad g_R^e = \sin^2 \theta_W$$

$$g_L^{\mu,\tau} = -\frac{1}{2} + \sin^2 \theta_W \qquad g_R^{\mu,\tau} = \sin^2 \theta_W$$

$$(4.5)$$

From Eq. (4.4) it is evident that if  $g_L^i g_R^i > 0$  there is a chance for the cross section to cancel in the physical region. From Eq. (4.5) we see that this zero is only possible in the  $\overline{\nu}_e e^- \rightarrow \overline{\nu}_e e^-$  channel and, in fact, it takes place for the kinematical configuration  $E_{\nu} = m_e/(4\sin^2\theta_W)$  and maximal T. Neither  $d\sigma^{\overline{\nu}_{\mu}}/dT$  nor  $d\sigma^{\overline{\nu}_{\tau}}/dT$  present a dynamical zero since  $g_L^{\mu,\tau} g_R^{\mu,\tau} < 0$ . We will take advantage of this fact.

In Fig. 2 we present the curves of constant values of  $d \equiv \log \left[\frac{d\sigma^{\overline{\nu}\mu}}{dT} / \frac{d\sigma^{\overline{\nu}e}}{dT}\right]$  (solid lines) in the plane  $(\theta, T)$  where the different regions where the appearance channel starts to be important<sup>3</sup>, that is when  $\frac{d\sigma^{\overline{\nu}\mu}}{dT} > \frac{d\sigma^{\overline{\nu}e}}{dT}$ , can be clearly seen. Curves of constant antineutrino energy are also shown (dashed lines).

Let us now consider the following observable:

$$R(\theta) = \frac{N(\theta)}{N_{U_{e3}=0}(\theta)}$$
(4.6)

where  $N(\theta)$  is the number of events for electron recoil angles smaller than  $\theta$  in the case of oscillations and  $N_{U_{e3}=0}(\theta)$  is the corresponding prediction for  $U_{e3} = 0$ . Close to the

<sup>&</sup>lt;sup>3</sup> The relation between  $\theta$  and the other two kinematic variables,  $E_{\overline{\nu}}$  and T, is given by  $\cos \theta = \frac{E_{\overline{\nu}} + m_e}{E_{\overline{\nu}}} \sqrt{\frac{T}{T + 2m_e}}$ .

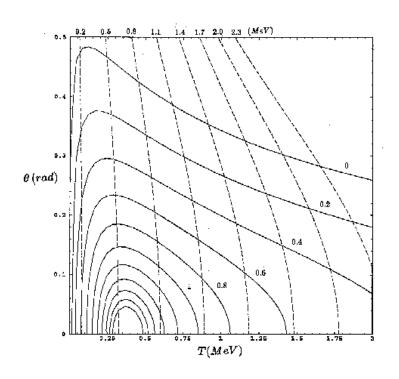


FIG. 2: Curves of constant values of  $d \equiv \log \left[\frac{\sigma^{\overline{\nu}\mu}}{dT} / \frac{d\sigma^{\overline{\nu}e}}{dT}\right]$  (solid lines) in the plane  $(\theta, T)$ . Curves of constant antineutrino energy are also plotted (dashed lines).

configuration of the dynamical zero (small  $\theta$  and the T-interval around  $T \simeq 2m_e/3$ ) R > 1 (appearance-like experiment), while if we consider a bigger sample R < 1 (disappearance-like experiment). This can be clearly seen by plotting  $R(\theta) - 1$  for different values of  $\theta = 0.3$  (solid line), 0.5 (dashed line) and  $1.11 \equiv \theta_{max}$  (dotted line) rad, as a function of  $\sin^2 2\theta_{13}$ , Fig. 3, for an electron recoil energy interval  $T \in [0.25, 0.80]$  MeV and for a reactor-detector baseline of L = 0.25 km.

As can be seen from Fig. 3, the region around the dynamical zero has a much better sensitivity to  $U_{e3}$  than in the case of making no angular selection. As expected, this is due to the fact that in that case, an appearance-like experiment is simulated, which is much more sensitive to small mixings than a disappearance-like one. Of course, when narrowing the angular detection window, the statistics is smaller. The immediate question one should

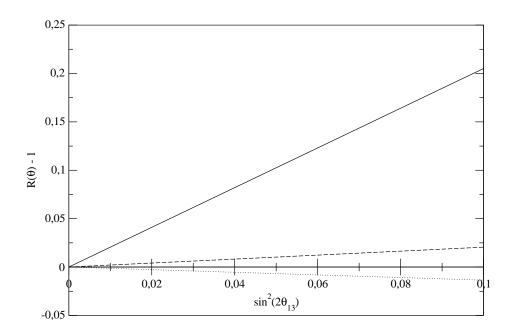


FIG. 3:  $R(\theta) - 1$  as a function of  $\sin^2 2\theta_{13}$ , for a given T-interval,  $T \in [0.25, 0.80]$  MeV, a reactordetector distance of 0.25 km, and for different values of  $\theta = 0.3$  rad (solid line), 0.5 rad (dashed line) and  $\theta_{max} = 1.11$  rad (dotted line).

wonder looking at Fig. 3 is whether this gain in sensitivity to  $\theta_{13}$  when considering small regions is large enough to compensate this decrease of statistics. It is important to notice that this high slope can be due to the ratio between two small quantities, being the denominator close to zero (it nearly vanishes over the dynamical zero). From Fig. 3, it can also be seen that there is an intermediate region where the effect of  $\overline{\nu}_e$  and  $\overline{\nu}_x$  interfere destructively and we have no sensitivity at all to  $\theta_{13}$ , even having much more statistics and independently of the value of  $\theta_{13}$ . This is clear from Eq. (4.3), for the term that depend on  $\theta_{13}$  will be suppressed when the effect of  $\frac{d\sigma^{\overline{\nu}_e}}{dT}(E_{\overline{\nu}_e},T)$  and  $\frac{d\sigma^{\overline{\nu}_x}}{dT}(E_{\overline{\nu}_e},T)$  compensate each other. Even if there are oscillations, at that configuration, the number of events is given just by  $d\sigma^{\overline{\nu}_e}/dT$ , and hence not being sensitive to oscillations. As seen from Eq. (4.3), the kinematics of that cancellation is given by the only condition that the charged current amplitude is twice the neutral current one, whereas the dynamical zero of the  $\overline{\nu}_e$  reaction shows up when the two interfering amplitudes are equal.

In order to estimate the bounds one could extract by measuring  $R(\theta)$ , we will assume that using the near detector to reduce systematics with the inverse  $\beta$ -decay reaction, lowers the uncertainty on the normalization of the reactor flux to  $\sigma_{sys} = 0.8\%$  [18]. Then, for a semi-

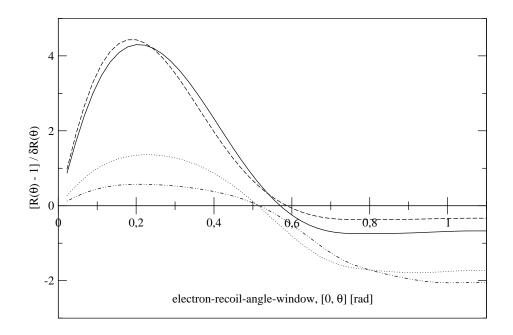


FIG. 4:  $(R(\theta) - 1)/\delta R(\theta)$  as a function of the electron recoil angle window (from 0 rad to  $\theta$  rad) for T  $\in [0.25, 0.80]$  MeV,  $\sin^2 2\theta_{13} = 0.04$  and a reactor-detector baseline of 0.17 km (dashed line), 0.25 km (solid line), 0.50 km (dotted line) and 0.75 km (dot-dashed line).

quantitative analysis, we will assume only statistical errors along with this systematic one associated to the normalization of the antineutrino spectrum. In Fig. 4,  $(R(\theta) - 1)/\delta R(\theta)$  is shown as a function of the electron-recoil-angle-window,  $\theta$ -window, within the T-interval, T  $\in [0.25, 0.80]$  MeV, for different reactor-detector distances and  $\sin^2 2\theta_{13} = 0.04$ . From Fig. 4, it is evident that if the entire  $\theta$ -window is considered (dissapearance regime), the sensitivity to small  $U_{e3}$  decreases as the reactor-detector distance decreases. On the contrary, this is the opposite to what happens within a  $\theta$ -window around the dynamical zero (appearance regime), the sensitivity increases as the reactor-detector distance decreases up to ~ 0.15–0.25 km.

These opposite behaviors can be understood by the fact that in the disappearance regime larger antineutrino energies play a role, and thus larger distances keep the oscillatory factor in the probability around its maximum. On the other hand, for antineutrino energies around the dynamical zero, this oscillatory maximum is reached at a reactor-detector distance of  $\sim 0.25$  km.

Comparatively, the best configuration for the appearance regime ( $\sim 0.25$  km) gives a

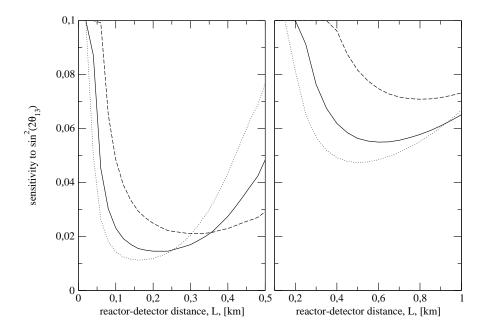


FIG. 5: Sensitivity to  $\sin^2 2\theta_{13}$  as a function of the reactor-detector baseline, L (in km), for different values of  $\Delta m_{31}^2 = 2 \times 10^{-3} \text{ eV}^2$  (dashed line),  $3 \times 10^{-3} \text{ eV}^2$  (solid line) and  $4 \times 10^{-3} \text{ eV}^2$  (dotted line), at the 90 % confidence level. The detection window is T  $\in [0.25, 0.80]$  MeV and:  $\theta \in [0, 0.25]$  rad (left plot) and for all  $\theta$  (right plot).

factor of two better in  $(R(\theta) - 1)/\delta R(\theta)$  than the best configuration for the disappearance regime (~ 0.75 km). For L = 0.25 km, sin<sup>2</sup>  $2\theta_{13} = 0.04$  would be resolved with a  $4\sigma$  confidence level in the appearance regime. For this configuration, a sensitivity down to sin<sup>2</sup>  $2\theta_{13} = 0.015$ could be reached at 90% confidence level, which is comparable to the sensitivity that can be reached using the inverse  $\beta$ -decay reaction in the far detector, sin<sup>2</sup>  $2\theta_{13} \sim 0.01$ . This is shown in the left plot of Fig. 5 where the sensitivity to sin<sup>2</sup>  $2\theta_{13}$  (largest value of sin<sup>2</sup>  $2\theta_{13}$  which fits the value sin<sup>2</sup>  $2\theta_{13} = 0$  at the chosen confidence level) is depicted as a function of the reactor-detector baseline, L (in km), for different values of  $\Delta m_{31}^2 = 2 \times 10^{-3}$  eV<sup>2</sup> (dashed line),  $3 \times 10^{-3}$  eV<sup>2</sup> (solid line) and  $4 \times 10^{-3}$  eV<sup>2</sup> (dotted line), at the 90 % confidence level. The detection window selected is  $\theta \in [0, 0.25]$  rad and T  $\in [0.25, 0.80]$  MeV. Thus, in what the dependence with  $\Delta m_{31}^2$  is concerned, there is a worse (better) sensitivity as it decreases (increases), within the allowed experimental range. For smaller values of  $\Delta m_{31}^2$  the sensitivity becomes slightly worse as the reactor-detector baseline becomes shorter (within L = 0.15-0.25 km), while for larger values of  $\Delta m_{31}^2$ , the best sensitivity is obtained at shorter

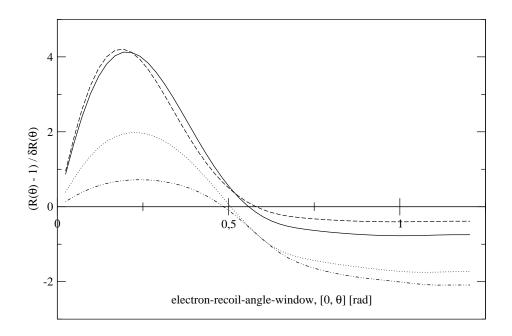


FIG. 6:  $(R(\theta) - 1)/\delta R(\theta)$  as a function of the electron-recoil-angle-window (from 0 rad to  $\theta$  rad) for T  $\in [0.15, 1.00]$  MeV,  $\sin^2 2\theta_{13} = 0.04$  and a reactor-detector baseline of 0.17 km (dashed line), 0.25 km (solid line), 0.50 km (dotted line) and 0.75 km (dot-dashed line).

baselines. The right plot in Fig. 5, analogous to the left one but with no  $\theta$ -window selected, i.e., counting all the events, shows in another way that the dissapearance channel is less sensitive for the allowed range of neutrino oscillation parameters. Thus, the knowledge of the kinematic region around the dynamical zero is of crucial importance in order to achieve a comparable sensitivity to the one in the far detector.

We can also study how the widening of the T-interval, keeping an angular-window fixed, affects the sensitivity. This is shown in Fig. 6, which is analogous to Fig. 4 but for  $T \in [0.15, 1.00]$  MeV. As we can see from the plot, considering slightly wider T-intervals does not affect significantly the sensitivity to  $U_{e3}$  while having more events. If we keep on widening the T-interval the sensitivity to  $U_{e3}$  within the appearance regime will decrease in a significant way for  $L \sim 0.15$ -0.25 km and will increase for  $L \gtrsim 0.5$  km. This occurs because of the contribution of higher energies and the displacement of the oscillation maximum to longer baselines. From a certain baseline,  $L \sim 0.75$  km, and up, the lack of events decreases the sensitivity. Thus, for a given  $\Delta m_{31}^2$ , there should be a compromise between narrowing the detection window in order to consider a region dominated by the dynamical zero (locating the detector at ~ 0.15-0.25 km) with a relative small number of events, and opening up this window in order to have a larger number of events, and then considering higher antineutrino energies having to move the detector to longer baselines, and consequently losing flux. We have found that the  $\theta$ -window, up to 0.2 - 0.3 rad, is demanded, whereas the recoil electron energy interval can be moderately extended at the expense of increasing the baseline. An appropriate choice appears for T  $\in [0.25, 0.80]$  MeV and L = 0.25 km.

#### V. CONCLUSIONS

Recent analyses have shown [17, 18] the interest of using two detectors in reactor neutrino oscillation experiments in order to reduce systematic errors and reach a sensitivity to the  $U_{e3}$ mixing comparable to the first-generation superbeams. Besides this strategy, we propose in this paper the use of the near detector to perform an appearance-like experiment by means of sitting around the dynamical zero in the  $\overline{\nu}_e - e$  elastic scattering cross section [20]. Although the cross section for  $\overline{\nu}_e + e^- \rightarrow \overline{\nu}_e + e^-$  is about 1% that of  $\overline{\nu}_e + p \rightarrow e^+ + n$ , the flux gain at smaller energies (around  $E_{\overline{\nu}_e} = 0.5$  MeV) and the corresponding shorter baseline of the near detector compensate this factor.

For a configuration with the near detector at ~ 0.25 km and a window in the electron recoil angle for  $\overline{\nu}_e + e^- \rightarrow \overline{\nu}_e + e^-$  from 0 to ~ 0.25 rad (for electron recoil kinetic energies up to ~ 1 MeV), we find a sensitivity down to  $\sin^2 2\theta_{13}$  which is comparable to the one that can be reached using the inverse  $\beta$ -decay reaction in the far detector at 1.7 km. In those windows for  $\overline{\nu}_e + e^- \rightarrow \overline{\nu}_e + e^-$ , the cross section for  $\overline{\nu}_x$  ( $x \neq e$ ) is larger than that for  $\overline{\nu}_e$  as can be seen in Fig. 2.

# ACKNOWLEDGMENTS

We thank Massimo Passera and Thomas Schwetz for useful discussions. This work is supported by the Spanish Grant FPA2002-00612 of the MCT. SPR has also been supported by the Spanish MECD for a FPU fellowship and by NASA Grant ATP02-0000-0151.

- K. Kaneyuki [SUPER-KAMIOKANDE Collaboration], Nucl. Phys. Proc. Suppl. 112 (2002) 24.
- [2] Q. R. Ahmad et al. [SNO Collaboration], Phys. Rev. Lett. 87 (2001) 071301; Q. R. Ahmad et al. [SNO Collaboration], Phys. Rev. Lett. 89 (2002) 011301; S. N. Ahmed et al. [SNO Collaboration], nucl-ex/0309004; S. Fukuda et al. [Super-Kamiokande Collaboration], Phys. Lett. B 539 (2002) 179.
- [3] K. Eguchi et al. [KamLAND Collaboration], Phys. Rev. Lett. 90 (2003) 021802.
- [4] S. N. Ahmed *et al.* [SNO Collaboration], nucl-ex/0309004.
- [5] P. I. Krastev and S. T. Petcov, Phys. Lett. B 205 (1988) 84; J. Arafune, M. Koike and J. Sato, Phys. Rev. D 56 (1997) 3093 [Erratum-ibid. D 60 (1999) 119905]; J. Bernabéu, Proc. WIN'99, World Scientific (2000), p. 227, hep-ph/9904474; K. Dick, M. Freund, M. Lindner and A. Romanino, Nucl. Phys. B 562 (1999) 29; J. Bernabéu and M. C. Bañuls, Nucl. Phys. Proc. Suppl. 87 (2000) 315.
- [6] M. C. Bañuls, G. Barenboim and J. Bernabéu, Phys. Lett. B 513 (2001) 391.
- [7] J. Bernabéu, S. Palomares-Ruiz, A. Pérez and S. T. Petcov, Phys. Lett. B 531 (2002) 90;
  J. Bernabéu and S. Palomares-Ruiz, PRHEP-hep2001/218, hep-ph/0112002; J. Bernabéu and
  S. Palomares-Ruiz, Nucl. Phys. Proc. Suppl. 110 (2002) 339, hep-ph/0201090.
- [8] J. Bernabéu, S. Palomares-Ruiz and S. T. Petcov, Nucl. Phys. B 669 (2003) 255.
- [9] C. Lunardini and A. Y. Smirnov, Nucl. Phys. B 616 (2001) 307; K. Takahashi and K. Sato, Phys. Rev. D 66 (2002) 033006; K. Takahashi and K. Sato, Prog. Theor. Phys. 109 (2003) 919; C. Lunardini and A. Y. Smirnov, JCAP 0306 (2003) 009; A. S. Dighe, M. T. Keil and G. G. Raffelt, JCAP 0306 (2003) 006.
- [10] M. Apollonio et al. [CHOOZ Collaboration], Phys. Lett. B 466 (1999) 415.
- [11] F. Boehm et al., Phys. Rev. D 64 (2001) 112001.
- [12] M. H. Ahn et al. [K2K Collaboration], Phys. Rev. Lett. 90 (2003) 041801.
- [13] D. Michael [MINOS Collaboration], Proceedings of the 20th International Conference on Neutrino Physics and Astrophysics, "Neutrino 2002", Munich, Germany, May 25-30.
- [14] S. Katsanevas [CNGS Collaboration], Proceedings of the 20th International Conference on

Neutrino Physics and Astrophysics, "Neutrino 2002", Munich, Germany, May 25-30.

- [15] Y. Itow et al., hep-ex/0106019; D. Ayres et al., hep-ex/0210005; A. Asratyan et al. hep-ex/0303023; H. Minakata and H. Nunokawa, JHEP 0110 (2001) 001; P. Huber, M. Lindner and W. Winter, Nucl. Phys. B 654 (2003) 3; J. J. Gómez-Cadenas et al. [CERN working group on Super Beams Collaboration], hep-ph/0105297; V. D. Barger, S. Geer, R. Raja and K. Whisnant, Phys. Rev. D 63 (2001) 113011; K. Whisnant, J. M. Yang and B. L. Young, Phys. Rev. D 67 (2003) 013004; G. Barenboim, A. De Gouvea, M. Szleper and M. Velasco, hep-ph/0204208; M. Mezzetto, J. Phys. G 29 (2003) 1781; B. Richter, hep-ph/0008222.
- [16] M. Apollonio *et al.*, hep-ph/0210192; A. De Rujula, M. B. Gavela and P. Hernandez, Nucl. Phys. B 547 (1999) 21; A. Cervera *et al.*, Nucl. Phys. B 579 (2000) 17 [Erratum-ibid. B 593 (2001) 731]; V. D. Barger, S. Geer, R. Raja and K. Whisnant, Phys. Rev. D 62 (2000) 073002; V. D. Barger, S. Geer, R. Raja and K. Whisnant, Phys. Rev. D 62 (2000) 013004.
- [17] H. Minakata, H. Sugiyama, O. Yasuda, K. Inoue and F. Suekane, Phys. Rev. D 68 (2003) 033017.
- [18] P. Huber, M. Lindner, T. Schwetz and W. Winter, Nucl. Phys. B 665 (2003) 487.
- [19] C. Bemporad, G. Gratta and P. Vogel, Rev. Mod. Phys. 74 (2002) 297.
- [20] J. Segura, J. Bernabéu, F. J. Botella and J. Peñarrocha, Phys. Rev. D 49 (1994) 1633.
- [21] P. Vogel and J. Engel, Phys. Rev. D **39** (1989) 3378.
- [22] F. T. Avignone and Z. D. Greenwood, Phys. Rev. C 22 (1980) 594; V. I. Kopeikin,
  L. A. Mikaelyan and V. V. Sinev, Phys. Atom. Nucl. 64 (2001) 849 [Yad. Fiz. 64 (2001) 914];
  H. V. Klapdor and J. Metzinger, Phys. Lett. B 112 (1982) 22; K. Schreckenbach, G. Colvin,
  W. Gelletly and F. Von Feilitzsch, Phys. Lett. B 160 (1985) 325; A. A. Hahn *et al.*, Phys.
  Lett. B 218 (1989) 365; O. Tengblad *et al.*, Nucl. Phys. A 503 (1989) 136.
- [23] G. Bellini [BOREXINO Collaboration], Proceedings of the 20th International Conference on Neutrino Physics and Astrophysics, "Neutrino 2002", Munich, Germany, May 25-30.
- [24] M. C. González-Garcia and C. Peña-Garay, Phys. Lett. B 527 (2002) 199,
- [25] Y. Declais *et al.*, Phys. Lett. B **338** (1994) 383.
- [26] F. Boehm and P. Vogel, The Physics of Massive Neutrinos, (New York, Cambridge University Press) 1992; H. Murayama and A. Pierce, Phys. Rev. D 65 (2002) 013012.
- [27] C. H. Llewellyn Smith, Phys. Rept. 3 (1972) 261; P. Vogel and J. F. Beacom, Phys. Rev. D 60 (1999) 053003; A. Strumia and F. Vissani, Phys. Lett. B 564 (2003) 42.

[28] J. Segura, J. Bernabéu, F. J. Botella and J. A. Peñarrocha, Phys. Lett. B **335** (1994) 93.